Acta Crystallographica Section F
Structural Biology and Crystallization Communications
ISSN 1744-3091

Cloning, expression, purification, crystallization and preliminary X-ray studies of the C-terminal domain of Rv3262 (FbiB) from *Mycobacterium tuberculosis*

Aisyah M. Rehan,[a,b,c]* Ghader Bashiri,[a,b] Neil G. Paterson,[a,b] Edward N. Baker[a,b] and Christopher J. Squire[a,b]

[a]Structural Biology Laboratory, School of Biological Sciences, The University of Auckland, Auckland, New Zealand, [b]Maurice Wilkins Centre for Molecular Biodiscovery, School of Biological Sciences, The University of Auckland, Auckland, New Zealand, and [c]Department of Biotechnology, Kulliyyah of Science, International Islamic University Malaysia, Kuantan, Pahang Malaysia

Correspondence e-mail: rais002@aucklanduni.ac.nz

Received 8 March 2011
Accepted 18 July 2011

During cofactor F_{420} biosynthesis, the enzyme F_{420}-γ-glutamyl ligase (FbiB) catalyzes the addition of γ-linked L-glutamate residues to form polyglutamylated F_{420} derivatives. In *Mycobacterium tuberculosis*, Rv3262 (FbiB) consists of two domains: an N-terminal domain from the F_{420} ligase superfamily and a C-terminal domain with sequence similarity to nitro-FMN reductase superfamily proteins. To characterize the role of the C-terminal domain of FbiB in polyglutamyl ligation, it has been purified and crystallized in an apo form. The crystals diffracted to 2.0 Å resolution using a synchrotron source and belonged to the tetragonal space group $P4_12_12$ (or $P4_32_12$), with unit-cell parameters $a = b = 136.6$, $c = 101.7$ Å, $\alpha = \beta = \gamma = 90^\circ$.

1. Introduction

The cofactor F_{420} is a flavin analogue that is essential for methanogenesis in archaea and is hypothesized to be important in the pathogenesis of *Mycobacterium tuberculosis* as a 'hydride carrier' owing to its lower redox potential compared with $NAD(P)^+$ (Boshoff & Barry, 2005). It has been suggested that under aerobic conditions this hydride carrier converts NO_2 released by *M. tuberculosis*-infected macrophages to NO. As NO_2 has been shown to be a more potent antimycobacterial agent, this might protect *M. tuberculosis* from nitrosative damage when it grows aerobically and causes active tuberculosis (Yu *et al.*, 1999; Purwantini & Mukhopadhyay, 2009). The importance of this cofactor has increased in significance with the increasing number of coenzyme F_{420}-dependent enzymatic reactions that have recently been identified in mycobacteria using comparative genomic methods (Selengut & Haft, 2010).

The open reading frame Rv3262 from *M. tuberculosis* encodes one of three enzymes that have been identified as being important in cofactor F_{420} biosynthesis in mycobacteria and is commonly termed FbiB ($\mathbf{F_{420}}$ **bi**osynthesis enzyme **B**; Choi *et al.*, 2001, 2002). FbiB is a multi-domain protein derived from the F_{420} ligase superfamily (N-terminal domain; Pfam PF01996; Eker *et al.*, 1990; Peschke *et al.*, 1995; Graupner & White, 2003; Nakano *et al.*, 2004) and the nitro-FMN reductase superfamily (C-terminal domain; Pfam PF00881; Hecht *et al.*, 1995; de Oliveira *et al.*, 2007) as indicated by sequence similarity. Following a series of biosynthetic reactions to form F_{420}, FbiB catalyzes the addition of γ-linked L-glutamate residues to form polyglutamylated F_{420} derivatives (Li, Graupner *et al.*, 2003). The length of the polyglutamate tail varies in different organisms. The majority of methanogenic and sulfate-reducing archaea predominantly have two glutamate residues, in which FbiB sequentially adds two γ-linked L-glutamate residues to F_{420}-0 (Nocek *et al.*, 2007). A γ-F_{420}-2-α-L-glutamyl ligase (CofF) caps the polyglutamate tail with a terminal α-linked glutamate in several methanogenic archaea (Li, Xu *et al.*, 2003).

In mycobacteria, the length of the polyglutamate tail varies by up to nine residues (Bair *et al.*, 2001; Bashiri *et al.*, 2008). The N-terminal domain of FbiB has 38% sequence identity to an archaeal F_{420}-γ-glutamyl ligase for which the structure has been determined (PDB entry 2g9i; Nocek *et al.*, 2007). The C-terminal domain of FbiB has 27% sequence identity to a nitroreductase from *M. smegmatis* (NfnB;

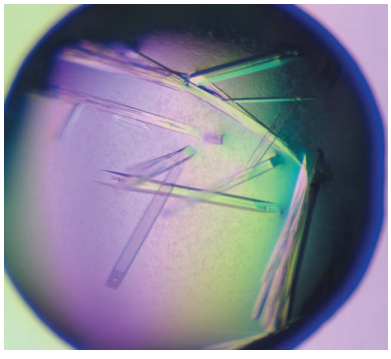

© 2011 International Union of Crystallography
All rights reserved

PDB entry 2wzw; Manina *et al.*, 2010), but it seems unlikely that its function is similar to that of NfnB, which inactivates antimycobacterial benzothiazinone drug molecules (Manina *et al.*, 2010). It is reasonable instead to hypothesize that the C-terminal domain of FbiB facilitates elongation of the polyglutamate tail of cofactor F_{420} in mycobacterial species and its function has been annotated as such (NCBI CDD TIGR03553). Here, we describe the structural characterization of this domain of FbiB, including its expression, purification, crystallization and preliminary X-ray diffraction analysis.

2. Materials and methods

2.1. Cloning, expression and purification

The open reading frame (ORF) encoding Rv3262 was amplified from *M. tuberculosis* H37Rv genomic DNA. Primers were designed for directional cloning of inserts into the Gateway cloning system (Invitrogen). The primer sequences were Rv3262_F5 (5′-GGC AGC GGC GCG ATG ACC GCC GAA GCG CTC-3′) and Rv3262_R5 (5′-GAA AGC TGG GTG TTA TCA CTT CAG GAT CAG CAA-3′). The open reading frame encoding residues 245–448 of Rv3262 was cloned into an expression plasmid with an amino-terminal His_6 tag, pDESTsmg (Goldstone *et al.*, 2008). For the Gateway cloning, a nested PCR with two rounds of amplification was performed. The first round of PCR used the gene-specific primers to amplify the gene of interest. The second PCR utilized the product from the first round of PCR as a template and used generic primers to incorporate the *att*B sites required for the Gateway BP recombination reaction. The subsequent PCR product was cloned into the pDONR221 vector (Invitrogen) by recombination using BP Clonase (Invitrogen).

The recombination product was transformed into *Escherichia coli* Top10 cells and plated onto LB agar plates supplemented with 50 µg ml^{-1} kanamycin. Positive *att*L-flanked entry clones containing the gene of interest were screened by *Bsr*GI restriction digest and sequencing. Positive clones were used in the subsequent recombination reaction with pDESTsmg and LR Clonase (Invitrogen) to generate an *M. smegmatis* expression plasmid. This construction resulted in the addition of a methionine at the first position of the amplified Rv3262-C gene and the addition of 32 extra residues at the N-terminus (MSHHHHHHLESPSTSLYKKAGFENLYFQGSGAM) of the recombinant protein. The LR recombination product was then transformed into *E. coli* Top10 cells and plated onto low-salt LB agar plates supplemented with 50 µg ml^{-1} hygromycin B for selection. Positive recombinant pDESTsmg plasmid clones were verified using *Bsr*GI digestion.

The expression construct was electroporated into *M. smegmatis* strain mc^{2}4517 following a published protocol (Bashiri *et al.*, 2010). Electrocompetent *M. smegmatis* mc^{2}4517 cells (40 µl) were mixed with 2 µl DNA in 0.2 cm cuvettes. A 260 µl volume of 10% glycerol was added to the mixture just before electroporation (electroporation parameters: R = 1000 Ω, Q = 25 µF and V = 2.5 kV; Bio-Rad Gene Pulser). After electroporation, the cells were immediately resuspended in 1 ml 7H9/ADC/Tween 80 solution (Difco and BBL Middlebrook). The cell suspension was incubated for 3 h at 310 K with shaking. The transformation was plated onto 7H10/ADC (Difco and BBL Middlebrook) agar plates supplemented with 50 µg ml^{-1} kanamycin and hygromycin B for selection.

The transformed His_6-FbiB-C (FbiB C-terminal domain) construct was expressed from the *M. smegmatis* culture using autoinduction medium (Studier, 2005) supplemented with 0.05% Tween 80 and 50 µg ml^{-1} each of kanamycin and hygromycin B. Fresh singly transformed colonies were inoculated in the non-inducing medium MDG (25 m*M* Na_2HPO_4, 25 m*M* KH_2PO_4, 50 m*M* NH_4Cl, 5 m*M* Na_2SO_4, 2 m*M* $MgSO_4$, 0.1× trace metals, 0.5% glucose, 0.25% aspartate). The MDG cultures were incubated for 48–72 h at 310 K while shaking at 200 rev min^{-1}. A 1:100 dilution of this culture was used to seed ZYM-5052 auto-induction medium (1% N-Z-amine AS, 0.5% yeast extract, 25 m*M* Na_2HPO_4, 25 m*M* KH_2PO_4, 50 m*M* NH_4Cl, 5 m*M* Na_2SO_4, 2 m*M* $MgSO_4$, 1× trace metals, 0.5% glycerol, 0.05% glucose, 0.2% α-lactose; Studier, 2005). The expression cultures were grown for 4 d at 310 K while shaking at 200 rev min^{-1} (Bashiri *et al.*, 2007). Cells were harvested by centrifugation (6800*g*, 20 min) and the cell pellets were kept at 253 K until use.

His_6-FbiB-C cell pellets were resuspended in lysis buffer (50 m*M* Tris pH 7.5, 100 m*M* NaCl, 2 m*M* β-mercaptoethanol) containing Complete Protease Inhibitor Cocktail Mini EDTA-free tablets (Roche) and passed twice through a cell disruptor at 17–18 kPa (Constant Systems Ltd). Insoluble matter was sedimented by centrifugation (17 000*g*, 40 min, 277 K). The soluble phase was filtered to 0.45 µm and loaded twice onto a HisTrap FF 5 ml nickel-affinity column (GE Healthcare) pre-equilibrated with wash buffer (lysis buffer plus 20 m*M* imidazole). The column was washed with at least ten column volumes of wash buffer before eluting the protein in a gradient of elution buffer (lysis buffer plus 500 m*M* imidazole). His_6-FbiB-C protein was eluted at approximately 160 m*M* imidazole. Following SDS–PAGE analysis, fractions containing the purified His_6-FbiB-C protein were pooled and dialyzed overnight into dialysis buffer (50 m*M* Tris pH 7.5, 100 m*M* NaCl, 2 m*M* β-mercaptoethanol) at 277 K.

The uncleaved His_6-FbiB-C protein was concentrated using a 3 kDa molecular-weight cutoff spin concentrator (GE Healthcare) before being subjected to size-exclusion chromatography on a Superdex 75 10/300 column (GE Healthcare) for the final purification step. The eluted protein fractions were analysed by 12 or 15% SDS–PAGE. Each gel-filtration fraction was assessed for heterogeneity using dynamic light scattering (Wyatt DynaPro Titan, Wyatt Technology Corporation).

2.2. Crystallization

The initial screening of crystallization conditions for native FbiB-C was performed at 291 K using a Cartesian nanolitre dispensing robot (Genome Solutions) and a locally compiled crystallization screen (Moreland *et al.*, 2005). The FbiB-C protein at a concentration of 15 mg ml^{-1} (in 50 m*M* Tris pH 7.5, 100 m*M* NaCl) was centrifuged at 16 000*g* for 15–30 min before setting up crystallization trays. Over 2–3 d, crystals were obtained from a variety of conditions. A grid screen using the hanging-drop vapour-diffusion technique and a reservoir volume of 500 µl was performed around several promising conditions. After optimization of the best screening conditions, X-ray diffraction-quality crystals were grown in hanging drops in 24-well plates (Hampton Research) containing 1–2 µl protein solution at 15 mg ml^{-1} and 1–2 µl precipitant solution that were equilibrated against 500 µl precipitant solution (20–25% PEG 3350, 0.20–0.35 *M* Li_2SO_4). Paratone oil and mineral oil (in a 70:30 ratio) was used as a cryoprotectant before flash-cooling the crystals in liquid nitrogen.

2.3. Data collection

X-ray diffraction data sets were collected from single crystals on the Australian Synchrotron MX2 beamline at a wavelength of 0.976233 Å using an ADSC Quantum 315r CCD detector. The crystal-to-detector distance was set to 250 mm, the oscillation range was 1.0° and 195 images were collected. Data were collected using the *Blu-Ice* software (McPhillips *et al.*, 2002), indexed and processed using *XDS* (Kabsch,

2010), reindexed using *POINTLESS* (Evans, 2006) and scaled with *SCALA* from the *CCP*4 program package (Evans, 2006; Winn *et al.*, 2011).

3. Results and discussion

FbiB-C was expressed in *M. smegmatis* cells and purified by IMAC and size-exclusion chromatography. Both size-exclusion chromatography and DLS showed that the protein was dimeric in solution (data not shown). His_6-FbiB-C protein eluted in a single peak was 99% pure based on SDS–PAGE and monodisperse in solution as indicated by DLS. Crystals grew readily by vapour diffusion in hanging-drop format to reach maximum dimensions of approximately 315 × 21 × 16 µm over several days. Larger crystals were obtained if the cover slides were deliberately poorly sealed to cause dehydration or if previous batches of crystals were seeded into fresh drops equilibrated overnight. Crystals of FbiB-C as shown in Fig. 1 diffracted to 2.0 Å resolution on the MX2 beamline at the Australian Synchrotron (Fig. 2). Data-collection statistics are given in Table 1. The crystals appeared to belong to the tetragonal crystal system, with unit-cell parameters $a = b = 136.6$, $c = 101.7$ Å, $\alpha = \beta = \gamma = 90^\circ$ and with potential space groups suggested as $P4_12_12$ or $P4_32_12$ from analysis of the systematic absences. The Matthews coefficient of 2.69 $Å^3$ Da^{-1} (Matthews, 1968) suggests the presence of four molecules per asymmetric unit with a solvent content of 54%. Self-rotation functions were calculated from the experimental data and from model coordinate systems (data not shown). The experimental self-rotation function is consistent with an asymmetric unit containing four molecules; specifically, two sets of dimers related by twofold NCS symmetry. Each dimer additionally displays internal twofold NCS symmetry.

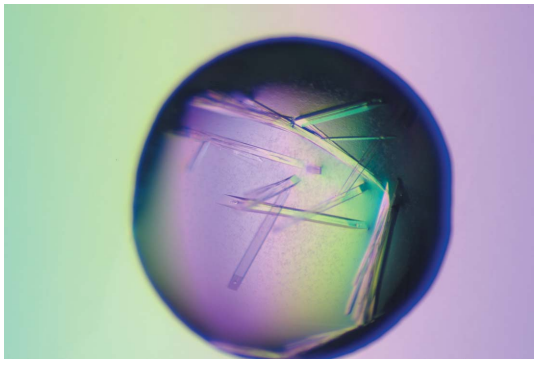

Figure 1
Crystals of FbiB-C (315 × 21 × 16 µm).

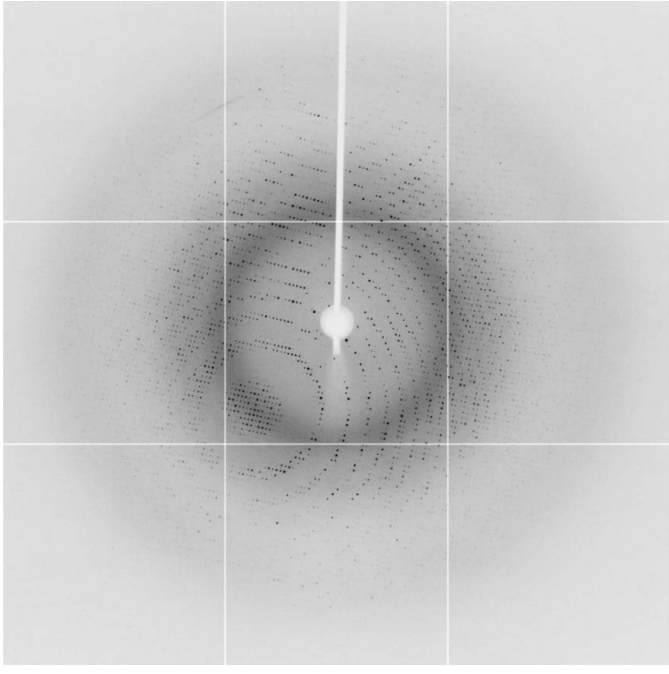

Figure 2
A typical diffraction image obtained from FbiB-C crystals.

Table 1
Crystal and data-collection statistics for FbiB-C.

Values in parentheses are for the highest resolution shell.

Space group	$P4_12_12$ or $P4_32_12$
Unit-cell parameters (Å, °)	$a = b = 136.6$, $c = 101.7$, $\alpha = \beta = \gamma = 90$
Resolution range (Å)	19.97–2.00 (2.11–2.00)
Total reflections	997618
Unique reflections	65279
Completeness (%)	99.9 (100.0)
Multiplicity	15.3 (14.5)
R_{merge}† (%)	11.2 (56.8)
$\langle I/\sigma(I)\rangle$	19.6 (5.2)

† $R_{merge} = \sum_{hkl}\sum_i |I_i(hkl) - \langle I(hkl)\rangle| / \sum_{hkl}\sum_i I_i(hkl)$, where $I_i(hkl)$ is the observed intensity and $\langle I(hkl)\rangle$ is the average intensity for multiple measurements.

We have been unable to solve the structure by molecular replacement to date; no suitable model was available or could be identified owing to the low sequence identity to currently known structures of this family (<27%). Phasing efforts are currently under way and the structure will be reported elsewhere.

This research was undertaken on the MX2 beamline at the Australian Synchrotron, Victoria, Australia. This research was supported by the Health Research Council of New Zealand and the Foundation for Research, Science and Technology of New Zealand. AMR is the recipient of a PhD scholarship from the IPTA Academic Training Scheme from the Ministry of Higher Education, Malaysia and International Islamic University Malaysia.

References

Bair, T. B., Isabelle, D. W. & Daniels, L. (2001). *Arch. Microbiol.* **176**, 37–43.
Bashiri, G., Rehan, A. M., Greenwood, D. R., Dickson, J. M. J. & Baker, E. N. (2010). *PLoS One*, **5**, e15803.
Bashiri, G., Squire, C. J., Baker, E. N. & Moreland, N. J. (2007). *Protein Expr. Purif.* **54**, 38–44.
Bashiri, G., Squire, C. J., Moreland, N. J. & Baker, E. N. (2008). *J. Biol. Chem.* **283**, 17531–17541.
Boshoff, H. I. & Barry, C. E. (2005). *Nature Rev. Microbiol.* **3**, 70–80.
Choi, K.-P., Bair, T. B., Bae, Y.-M. & Daniels, L. (2001). *J. Bacteriol.* **183**, 7058–7066.
Choi, K.-P., Kendrick, N. & Daniels, L. (2002). *J. Bacteriol.* **184**, 2420–2428.
Eker, A. P., Kooiman, P., Hessels, J. K. & Yasui, A. (1990). *J. Biol. Chem.* **265**, 8009–8015.
Evans, P. (2006). *Acta Cryst.* D**62**, 72–82.
Goldstone, R. M., Moreland, N. J., Bashiri, G., Baker, E. N. & Lott, J. S. (2008). *Protein Expr. Purif.* **57**, 81–87.
Graupner, M. & White, R. H. (2003). *J. Bacteriol.* **185**, 4662–4665.
Hecht, H.-J., Erdmann, H., Park, H. J., Sprinzl, M. & Schmid, R. D. (1995). *Nature Struct. Biol.* **2**, 1109–1114.
Kabsch, W. (2010). *Acta Cryst.* D**66**, 125–132.
Li, H., Graupner, M., Xu, H. & White, R. H. (2003). *Biochemistry*, **42**, 9771–9778.
Li, H., Xu, H., Graham, D. E. & White, R. H. (2003). *Proc. Natl Acad. Sci. USA*, **100**, 9785–9790.
Manina, G. *et al.* (2010). *Mol. Microbiol.* **77**, 1172–1185.

Matthews, B. W. (1968). *J. Mol. Biol.* **33**, 491–497.
McPhillips, T. M., McPhillips, S. E., Chiu, H.-J., Cohen, A. E., Deacon, A. M., Ellis, P. J., Garman, E., Gonzalez, A., Sauter, N. K., Phizackerley, R. P., Soltis, S. M. & Kuhn, P. (2002). *J. Synchrotron Rad.* **9**, 401–406.
Moreland, N., Ashton, R., Baker, H. M., Ivanovic, I., Patterson, S., Arcus, V. L., Baker, E. N. & Lott, J. S. (2005). *Acta Cryst.* D**61**, 1378–1385.
Nakano, T., Miyake, K., Endo, H., Dairi, T., Mizukami, T. & Katsumata, R. (2004). *Biosci. Biotechnol. Biochem.* **68**, 1345–1352.
Nocek, B., Evdokimova, E., Proudfoot, M., Kudritska, M., Grochowski, L. L., White, R. H., Savchenko, A., Yakunin, A. F., Edwards, A. & Joachimiak, A. (2007). *J. Mol. Biol.* **372**, 456–469.
Oliveira, I. M. de, Henriques, J. A. & Bonatto, D. (2007). *Biochem. Biophys. Res. Commun.* **355**, 919–925.
Peschke, U., Schmidt, H., Zhang, H.-Z. & Piepersberg, W. (1995). *Mol. Microbiol.* **16**, 1137–1156.
Purwantini, E. & Mukhopadhyay, B. (2009). *Proc. Natl Acad. Sci. USA*, **106**, 6333–6338.
Selengut, J. D. & Haft, D. H. (2010). *J. Bacteriol.* **192**, 5788–5798.
Studier, F. W. (2005). *Protein Expr. Purif.* **41**, 207–234.
Winn, M. D. *et al.* (2011). *Acta Cryst.* D**67**, 235–242.
Yu, K., Mitchell, C., Xing, Y., Magliozzo, R. S., Bloom, B. R. & Chan, J. (1999). *Tuber. Lung Dis.* **79**, 191–198.